Electronic Supplementary Material (ESI) for Materials Chemistry Frontiers.

"Supporting Information"

Tris-tetrazole based nanostructured soft material: studies on self-healing, AIEE, rheological and fluorometric detection of 3-aminopyridine

Reena Kyarikwal,[a] Bidyut Kumar Kundu,[a,b] Argha Chakraborty[a] and Suman Mukhopadhyay[a]*

[a]Department of Chemistry, School of basic science, Indian Institute of Technology Indore, Khandwa road, Simrol, Indore, 453552, India

[b]Department of Chemistry, University of Cincinnati, Cincinnati, Ohio, 45221, United States

*E-mail: suman@iiti.ac.in. Phone: +91 731 2438 735. Fax: +91 731 2361 482

Table of Contents

Fig. S19: (a) Fluorescence spectra of G8-3AP at different concentration ratio in DMSO: CH_3CH_2OH (b) Job's plot to shows the ratio of amount of interaction of G8-3AP at maximum intensity.

Fig. S20: (a) Fluorescence spectra of G8-3AP at different concentration ratio in DMSO: CH_3CN (b) Job's plot to shows the ratio of amount of interaction of G8-3AP at maximum intensity.

Fig. S21: (a) Fluorescence spectra of G8-3AP at different concentration ratio in DMSO: CH_3Cl (b) Job's plot to shows the ratio of amount of interaction of G8-3AP at maximum intensity.

Fig. S22: (a) Fluorescence spectra of G8-3AP at different concentration ratio in DMSO: $CH_3COOCH_2CH_3$ (b) Job's plot to shows the ratio of amount of interaction of G8-3AP at maximum intensity.

Table S4: Bond lengths and bond angles of structure of planer G8 Molecule from DFT Data.

Fig. S23: HOMO-LUMO energy orbitals of gelator molecule G8 studied by DFT analysis.

Fig. S24: Predicted structure demonstration of organogel **G8-2AP and G8-3AP** by DFT study.

Table S5: Comparative study of rheology of organogels G8, G8-2AP, G8-3AP and G8-4AP.

Fig. S25: (a) LVE Angular sweep (AS) and (b) Frequency sweep (FS) of organogel G8.

Fig. S26: (a) LVE Angular sweep (AS) and (b) Frequency sweep (FS) of organogel G8-2AP.

Fig. S27: (a) LVE Angular sweep (AS) and (b) Frequency sweep (FS) of organogel G8-3AP.

Fig. S28: (a) LVE Angular sweep (AS) and (b) Frequency sweep (FS) of organogel G8-4AP.

Fig. S29: FE-SEM images of (a) Organogel G8 and (b) Xerogel of Organogel G8 at 200 nm.

Fig. S30: FE-SEM images of (a) Organogel G8-2AP and (b) Xerogel of Organogel G8-2AP at 200 nm.

Fig. S31: FE-SEM images of (a) Organogel G8-3AP and (b) Xerogel of Organogel G8-3AP at 200 nm.

Fig. S32: FE-SEM images of (a) Organogel G8-4AP and (b) Xerogel of Organogel G8-4AP at 200 nm.

Fig. S33: FT-IR data of xerogel of G8, G8-2APX, G8-3APX and G8-4APX.

Table S6: Comparative wavenumber range to show the participation of amine and tetrazolic ring for gelation.

Fig. S34: PXRD data of (a) gelator powder G8 and Xerogel of (b) G8, (c) G8-2AP, (d) G8-3AP, (e)G8-4AP.

Fig. S35: TGA data of gelator molecule G8 and xerogels of organogels of G8, G8-2AP, G8-3AP and G8-4AP.

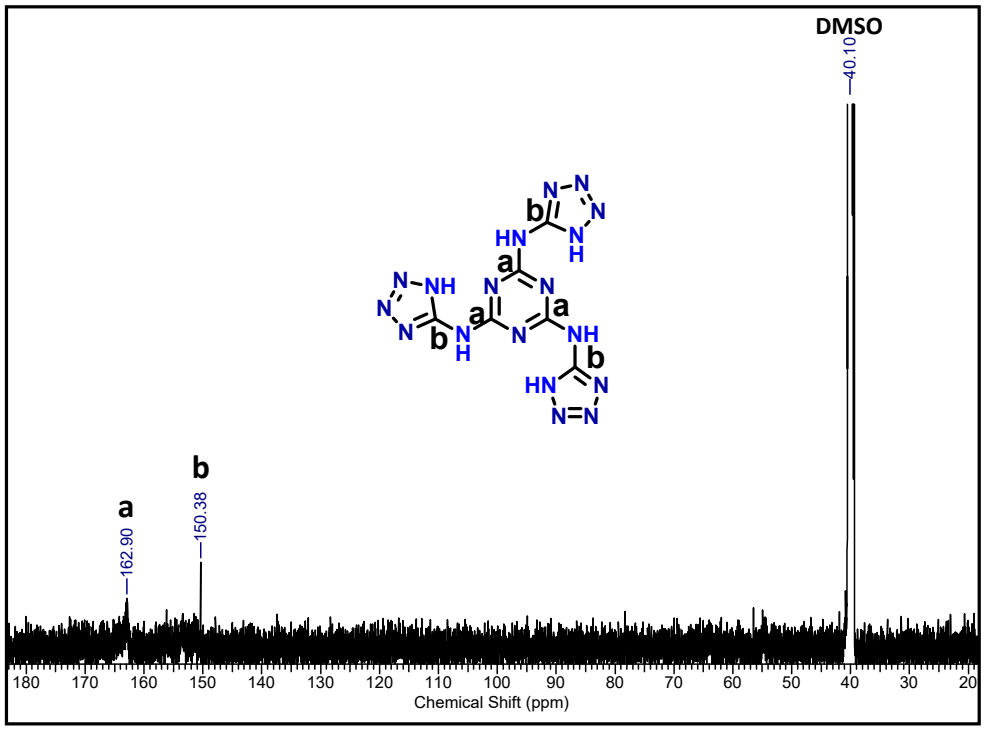

Fig. S1: ^{13}C NMR of gelator G8.

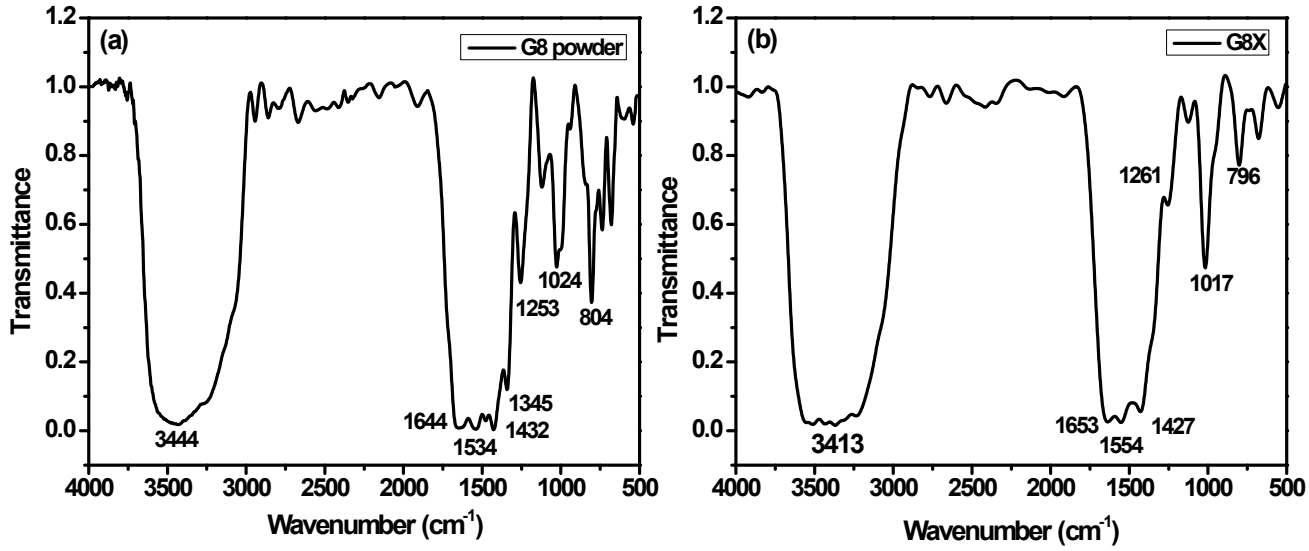

Fig. S2: FT-IR data of gelator powder G8 and xerogel of G8.

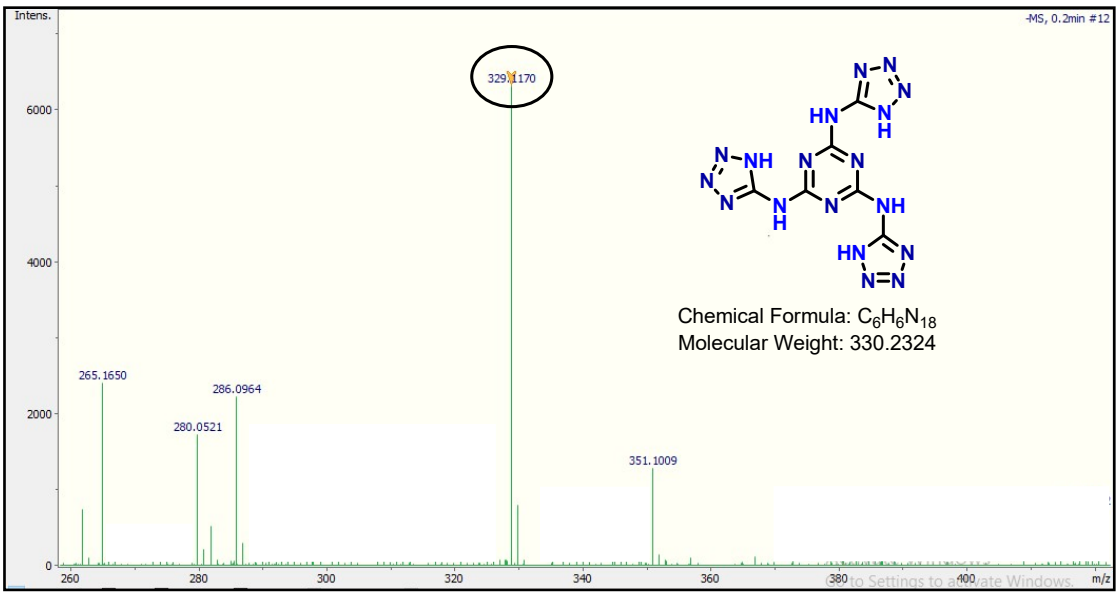

Fig. S3: ESI-MS of gelator G8.

Table S1: Solubility of G8 with different organic solvent. **I:** Insoluble, **S:** Soluble, **G:** Gelation.

Solvent	Solubility (G8)	Gelation	Solvent	Solubility	Gelation
Cyclohexane	I	-	Toluene	I	-
THF	I	-	Methanol	I	-
N-Hexane	I	-	DMF	**S after heating**	**G**
Acetone	I	-	Chloroform	I	-
Petroleum ether	I	-	Dichloromethane	I	-
Ethyl Acetate	I	-	DMSO	**S**	**G**
Benzene	I	-	Ethanol	I	-

Table S2: Optimization table of gelation condition of G8.

Concentration	DMSO/ H_2O	Gelation
17 mM	1 mL/1mL	No
34 mM	1 mL/1mL	Yes (Week gel)
50 mM	**1 mL/1mL**	**Yes (Strong gel)**
68 mM	1 mL/1mL	Yes (Strong but opaque gel)
85 mM	1 mL/1mL	Yes (Very strong but opaque gel)

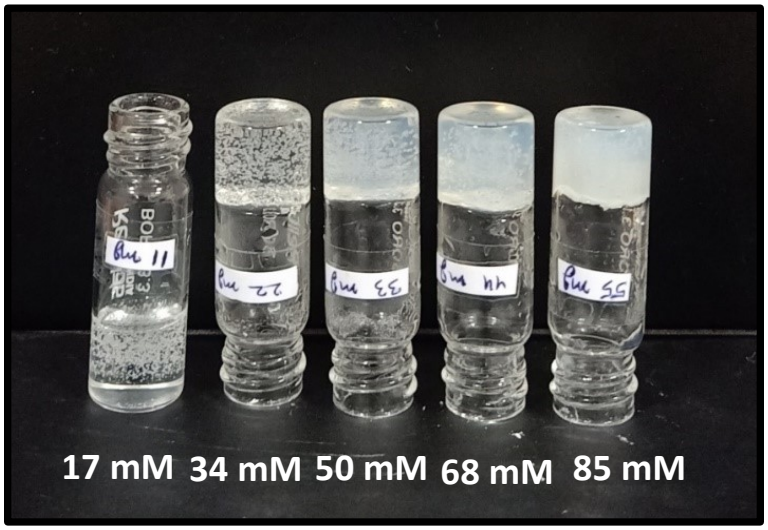

Fig. S4: Optimization of gelation condition of G8.

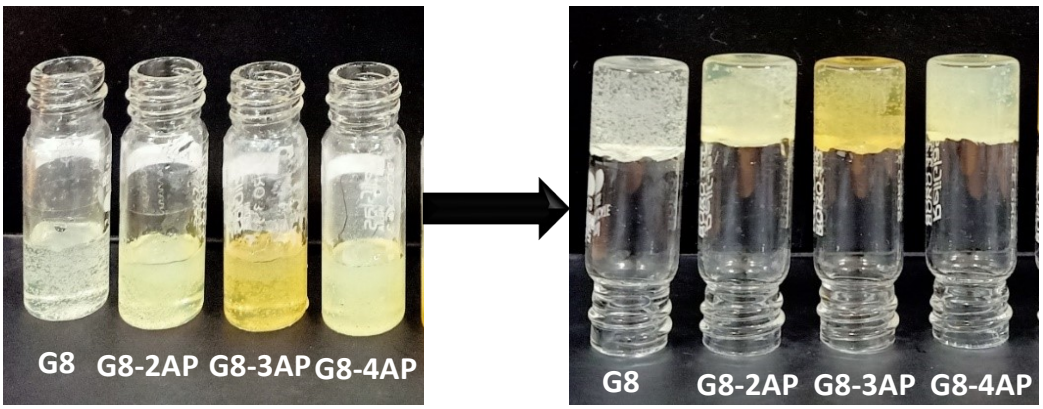

Fig. S5: Confirmation of gel formation by test tube inversion method.

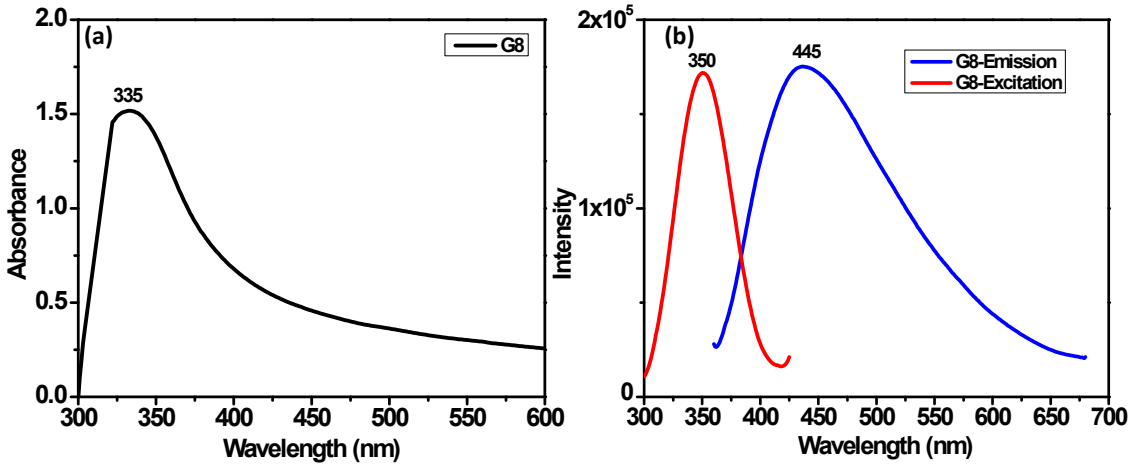

Fig. S6: (a) Solid state UV-Vis analysis of G8 (b) Excitation and emission wavelength of G8 by fluorometer.

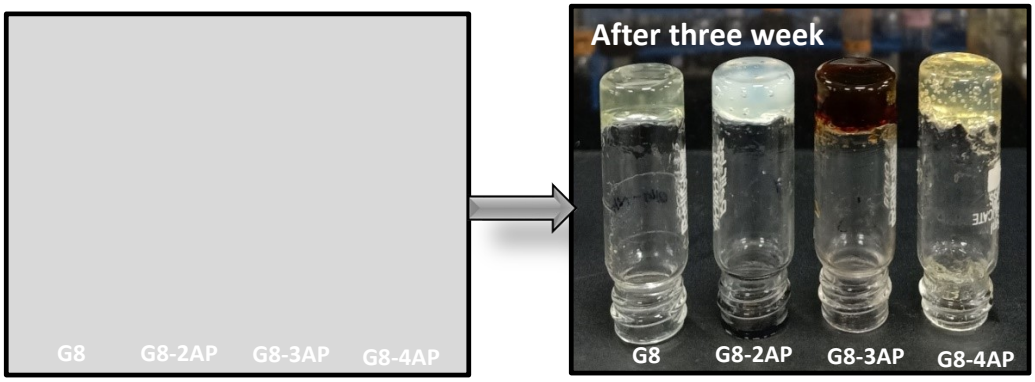

Fig. S7: Notable Colour change of **G8-3AP** organogel after three week at normal condition.

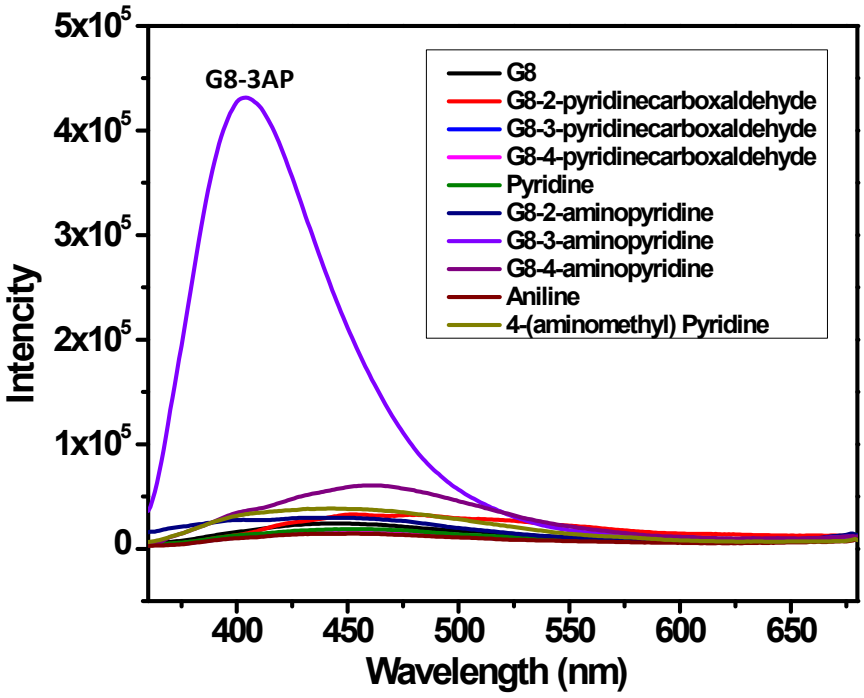

Fig. S8: Fluorescence experiments for interaction of **G8** with different pyridine compounds.

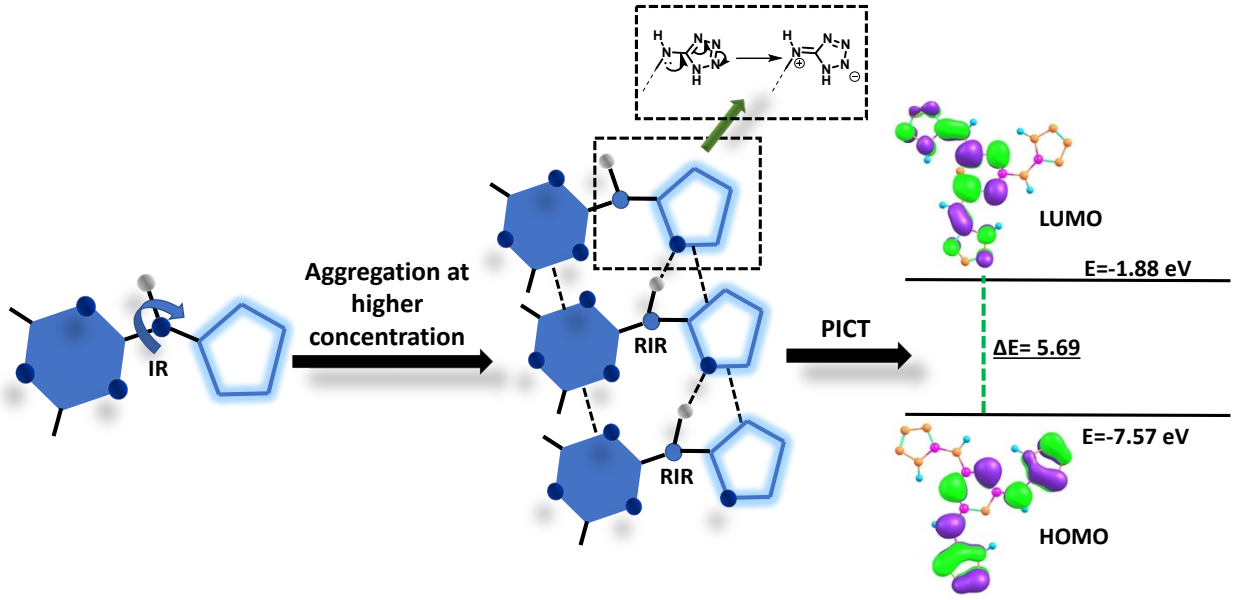

Fig. S9: Schematic representation of intramolecular charge transfer in planar molecule **G8**

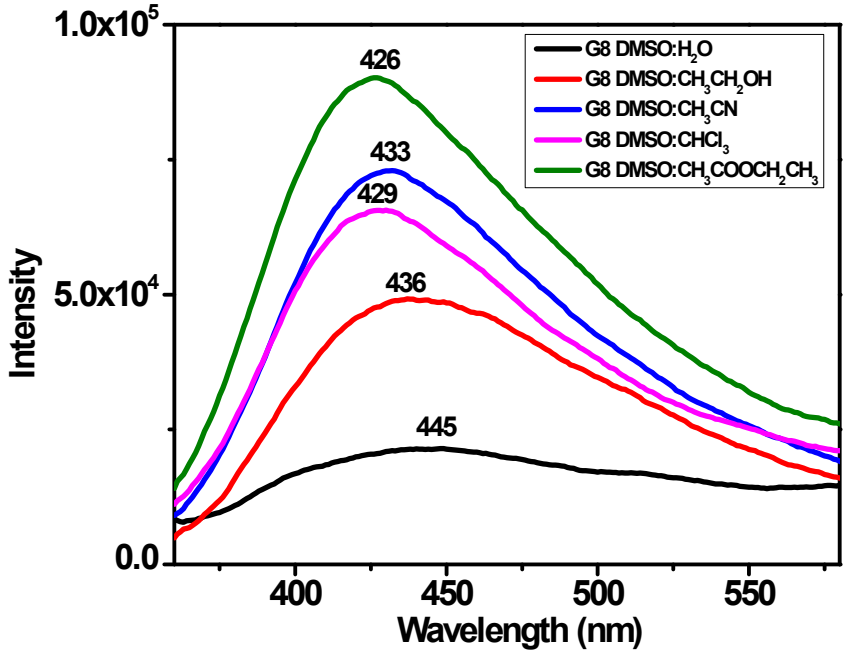

Fig. S10: Effect of solvent on wavelength of G8 molecule.

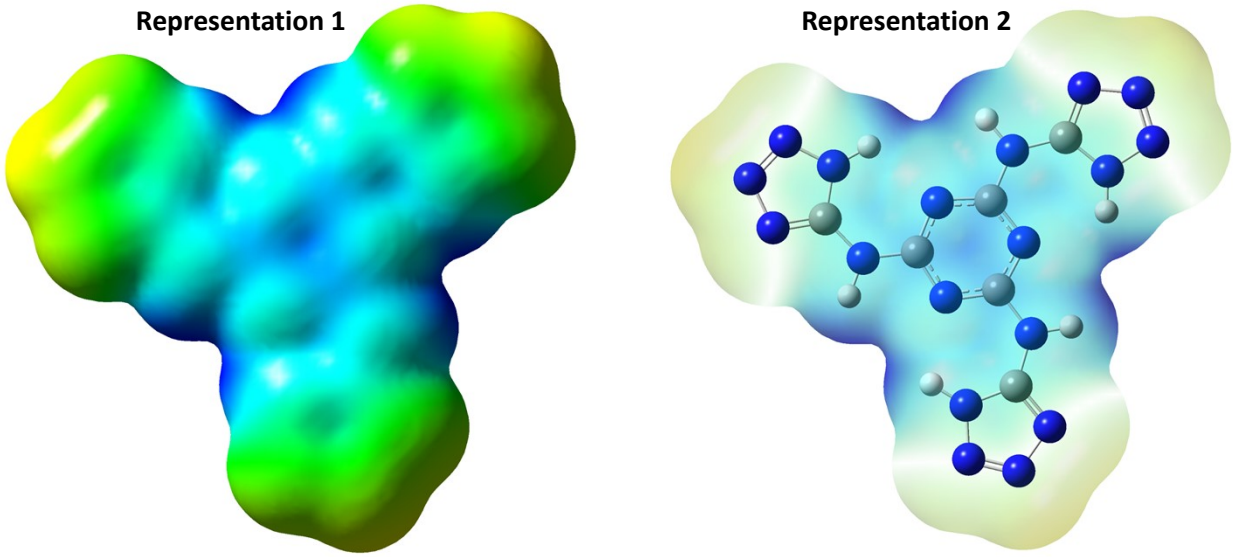

Fig. S11: G8 molecule Mapped with ESP.

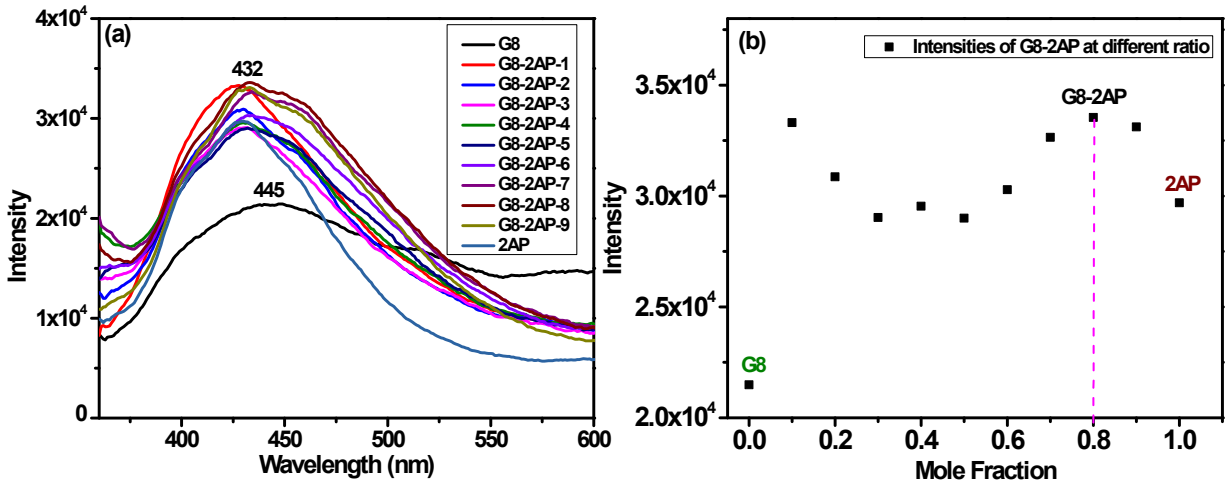

Fig. S12: (a) Fluorescence spectra of G8-2AP at different concentration ratio (b) Job's plot to shows the maximum intensity ratio of G8-2AP.

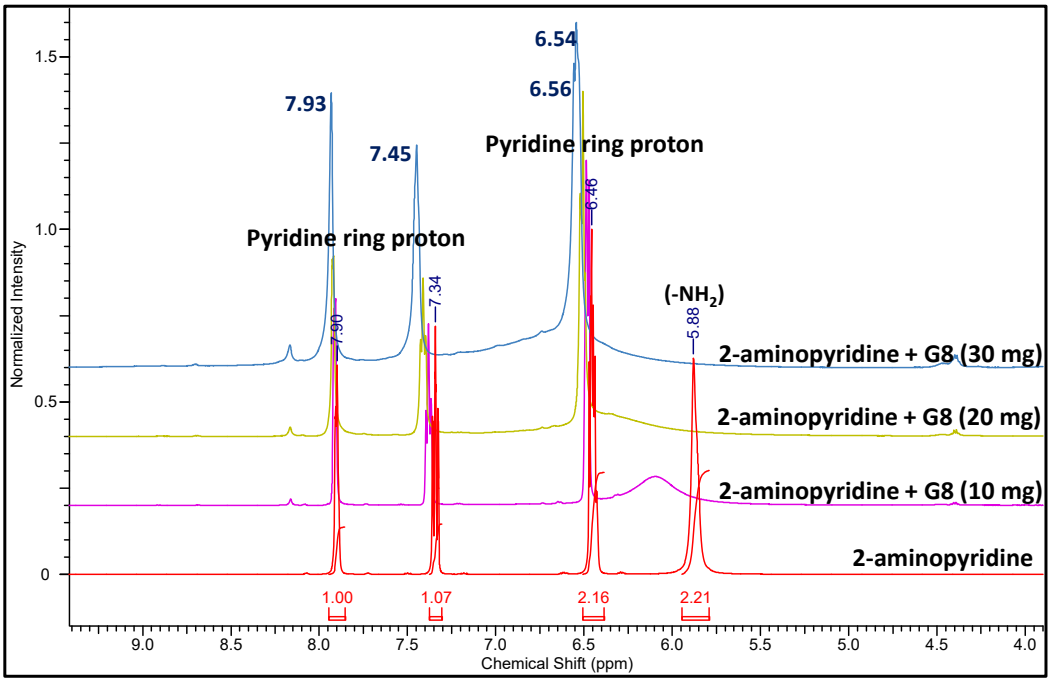

Fig. S13: Concentration dependent ^{1}H NMR of 2-aminopyriine with increasing amount of gelator molecule G8 showing participation of hydrogen and nitrogen for hydrogen bonding.

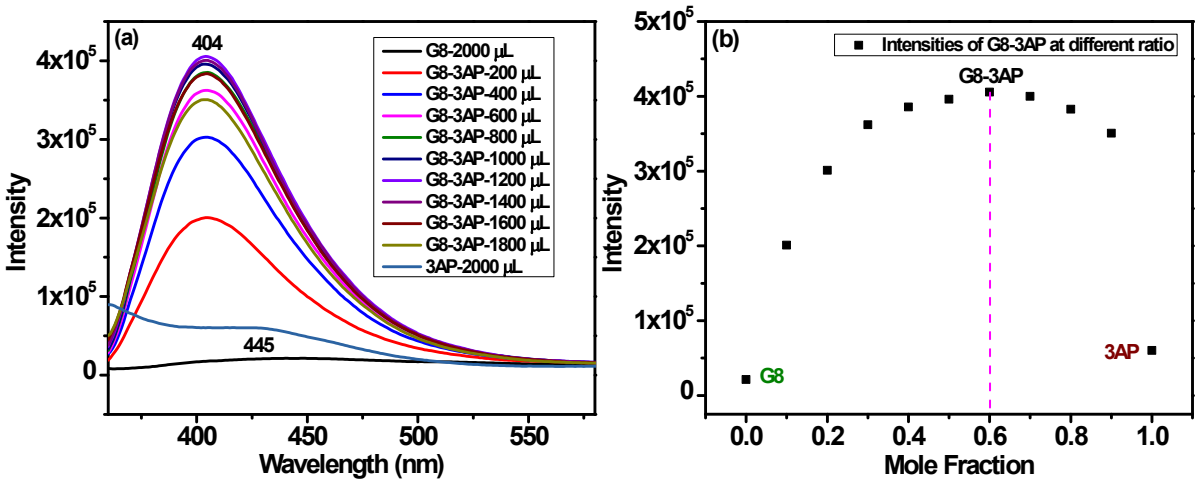

Fig. S14: (a) Fluorescence spectra of G8-3AP at different concentration ratio (b) Job's plot to shows the maximum intensity ratio of G8-3AP.

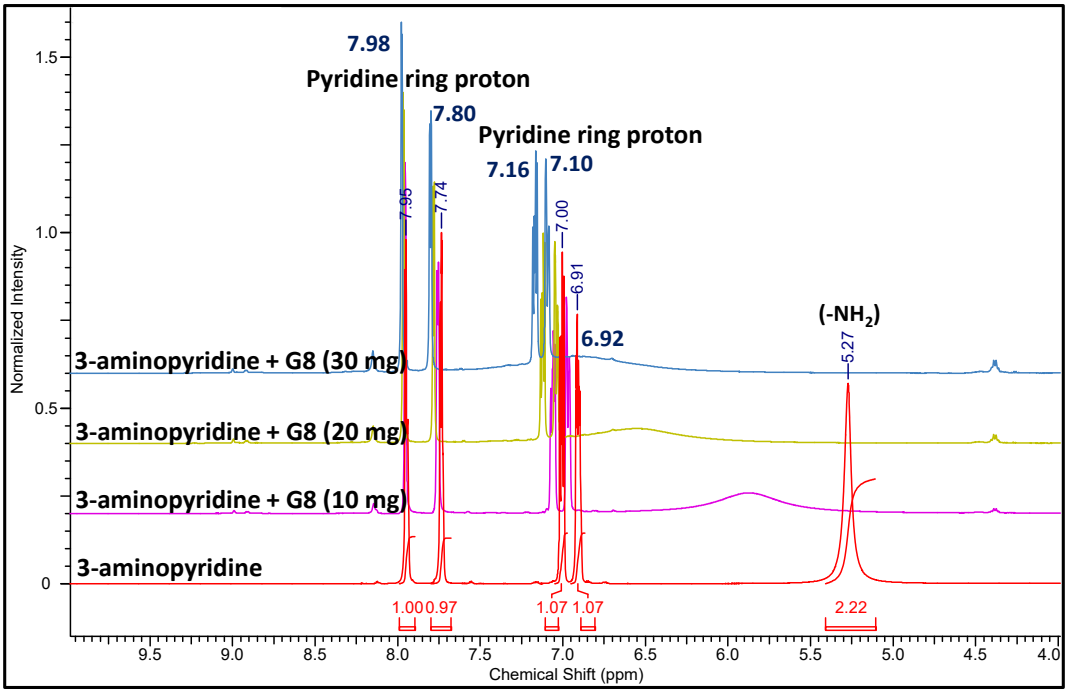

Fig. S15: Concentration dependent ^{1}H NMR of 3-aminopyriine with increasing amount of gelator molecule G8 showing participation of hydrogen and nitrogen for hydrogen bonding.

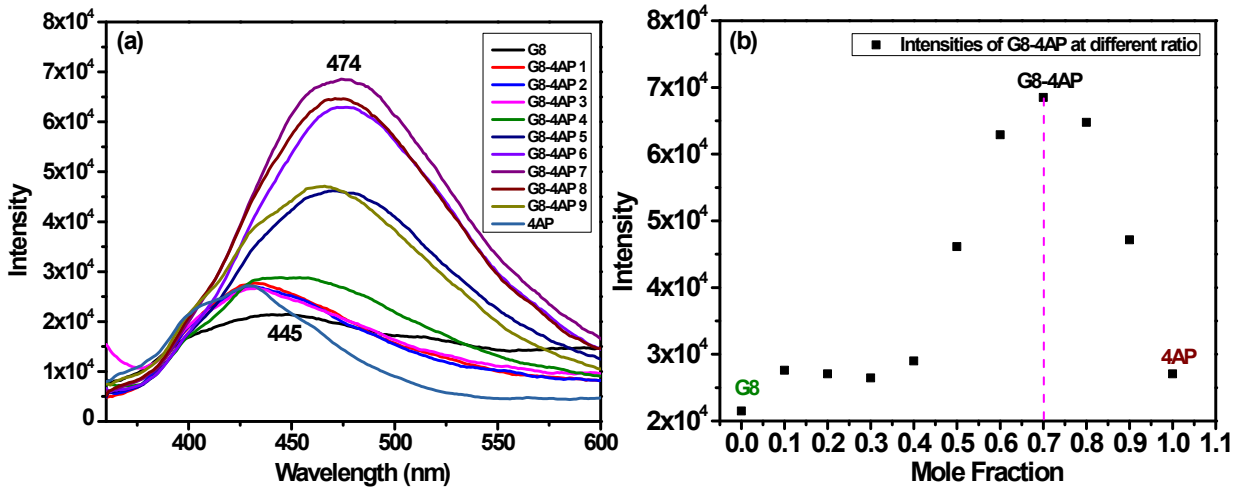

Fig. S16: (a) Fluorescence spectra of G8-4AP at different concentration ratio (b) Job's plot to shows the maximum intensity ratio of G8-4AP.

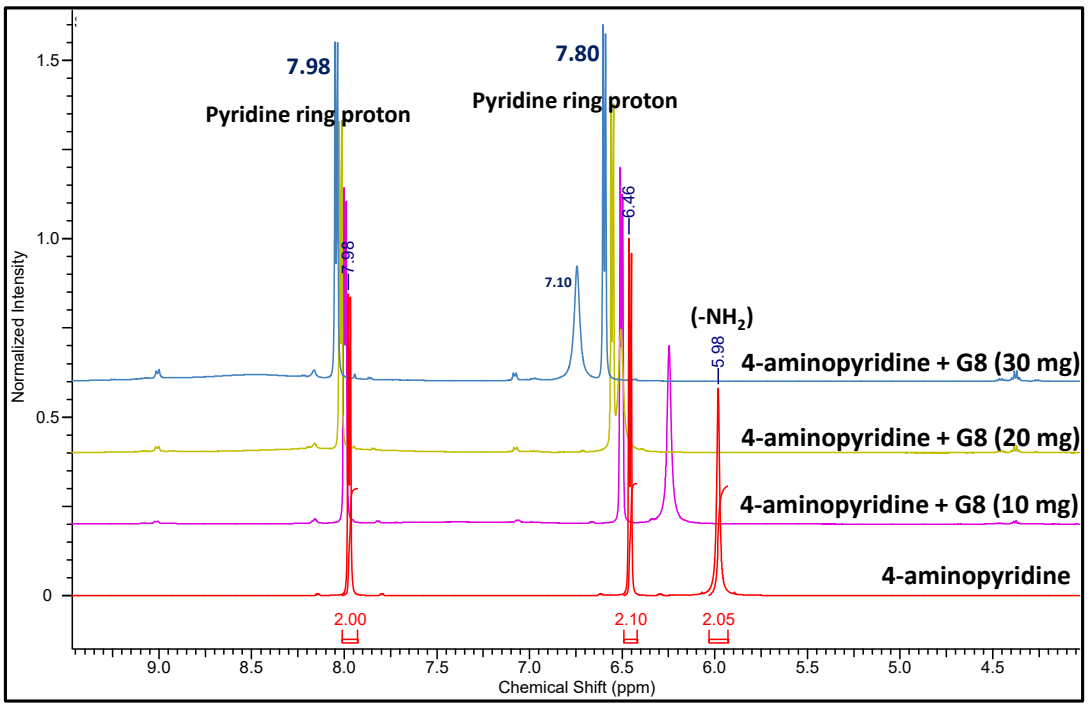

Fig. S17: Concentration dependent ^{1}H NMR of 4-aminopyriine with increasing amount of gelator molecule G8 showing participation of hydrogen and nitrogen for hydrogen bonding.

Table S3: ^{1}H NMR data of downward shifting of protons of 2-aminopyridine, 3-aminopyridine and 4-aminpyridine during interactions with gelator molecule G8.

2-AP (212 mM)	**G8 (60 mM)**	**G8 (120 mM)**	**G8 (180 mM)**
7.90 ppm (aromatic)	7.91	7.93	7.93
7.34 ppm (aromatic)	7.38	7.41	7.45
6.46 ppm (aromatic)	6.49	6.51	6.54
5.88 ppm (-NH_2)	6.10	6.50	**6.56**
3-AP (212 mM)	**G8 (60 mM)**	**G8 (120 mM)**	**G8 (180 mM)**
7.95 (aromatic)	7.96	7.97	7.98
7.74 (aromatic)	7.75	7.78	7.80
7.00 (aromatic)	7.06	7.12	7.16
6.91 (aromatic)	6.98	7.05	**7.10**
5.27 (-NH_2)	5.86	6.55	**6.92**
4-AP (212 mM)	**G8 (60 mM)**	**G8 (120 mM)**	**G8 (180 mM)**
7.98 (aromatic)	8.00	8.01	8.05
6.46 (aromatic)	6.51	6.56	6.60
5.98 (-NH_2)	6.25	6.51	**6.74**

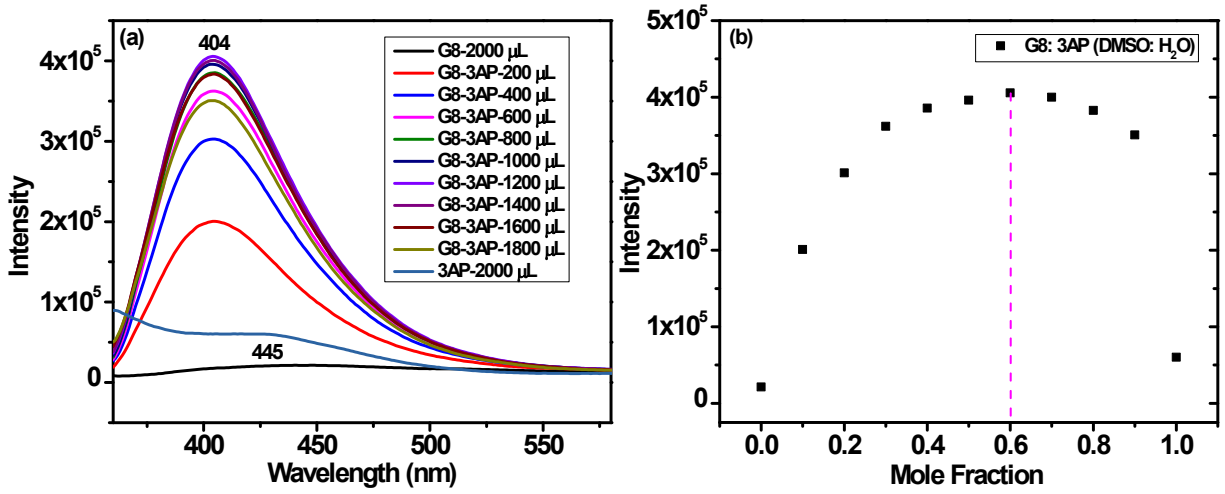

Fig. S18: (a) Fluorescence spectra of G8-3AP at different concentration ratio in DMSO: H_2O (b) Job's plot to shows the ratio of amount of interaction of G8-3AP at maximum intensity.

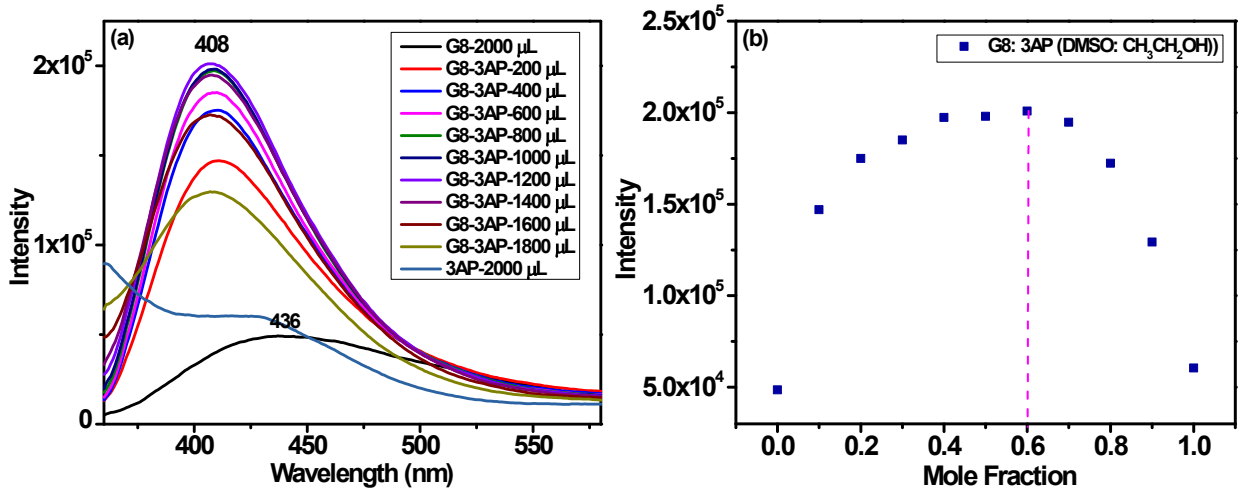

Fig. S19: (a) Fluorescence spectra of G8-3AP at different concentration ratio in DMSO: CH_3CH_2OH (b) Job's plot to shows the ratio of amount of interaction of G8-3AP at maximum intensity.

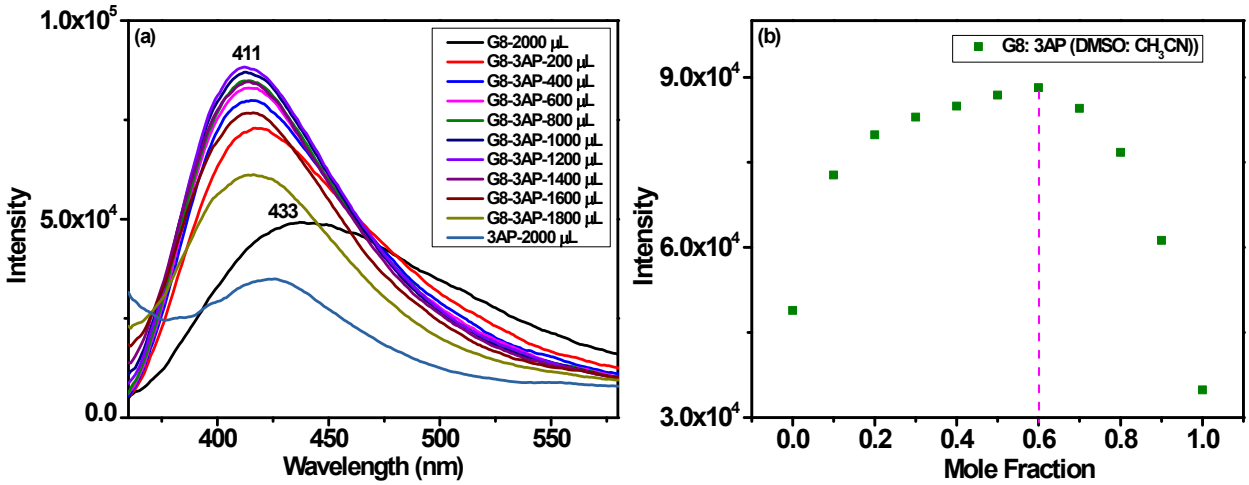

Fig. S20: (a) Fluorescence spectra of G8-3AP at different concentration ratio in DMSO: CH_3CN (b) Job's plot to shows the ratio of amount of interaction of G8-3AP at maximum intensity.

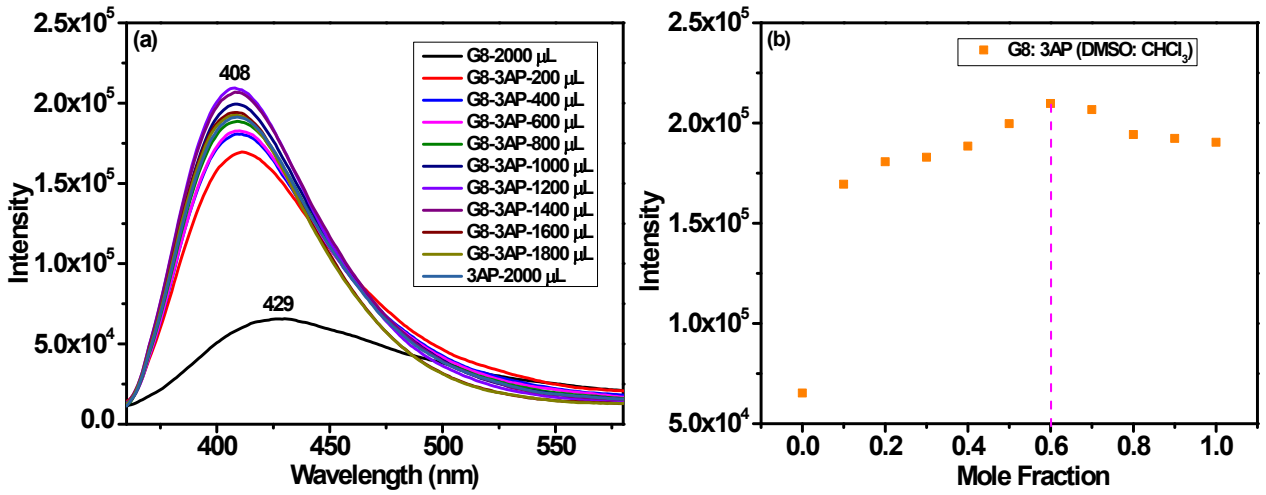

Fig. S21: (a) Fluorescence spectra of G8-3AP at different concentration ratio in DMSO: CH_3Cl (b) Job's plot to shows the ratio of amount of interaction of G8-3AP at maximum intensity.

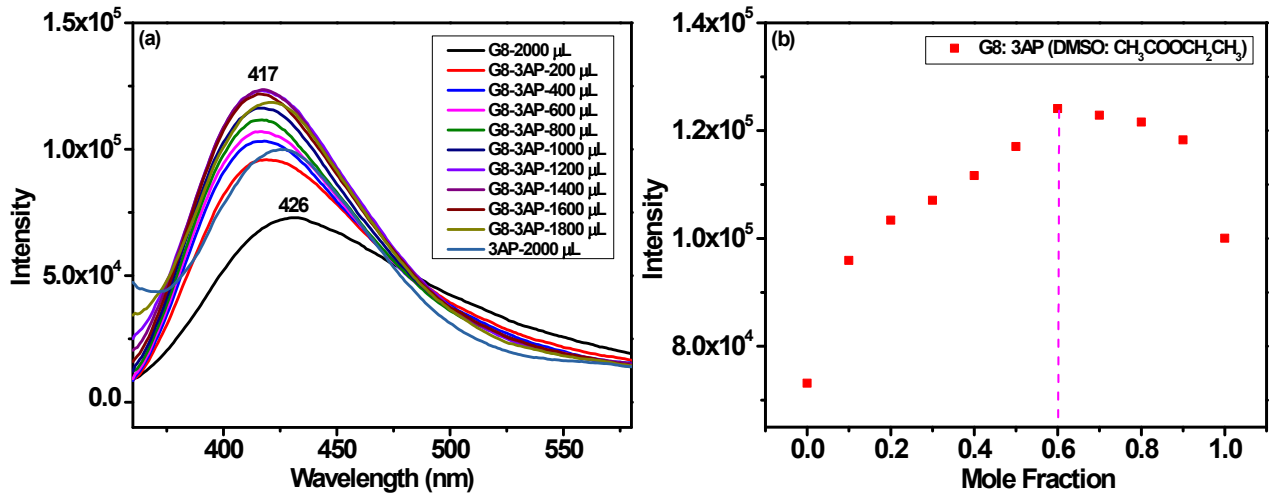

Fig. S22: (a) Fluorescence spectra of G8-3AP at different concentration ratio in DMSO: $CH_3COOCH_2CH_3$ (b) Job's plot to shows the ratio of amount of interaction of G8-3AP at maximum intensity.

Table S4: Bond lengths and bond angles of structure of planer **G8** molecule from DFT Data.

Molecule	Bond	Bond Length (Å)	Bond	Bond Length (Å)	Bond Name	Bond Angel (°)
G8	C1-N1	1.33	N5-C5	1.37	N3-C1-N4	115.37
	N1-C2	1.34	C5-N11	1.32	N1-C1-N4	118.67
	C2-N2	1.33	N11-N12	1.36	C1-N4-C4	127.12
	N2-C3	1.34	N12-N13	1.29	N4-C4-N10	127.22
	C3-N3	1.33	N13-N14	1.35	N2-C2-N5	115.38
	N3-C1	1.34	N14-H5	1.01	N1-C2-N5	118.67
	C1-N4	1.37	N14-C6	1.34	C2-N5-C5	127.09
	N4-H1	1.01	C3-N6	1.37	N5-C5-N14	127.20
	N4-C4	1.37	N6-H3	1.01	N3-C3-N6	115.38
	C4-N7	1.32	N6-C6	1.37	N2-C3-N6	188.66
	N7-N8	1.36	C6-N15	1.32	C3-N6-C6	127.11
	N8-N9	1.29	N15-N16	1.36	N6-C6-N18	127.20
	N9-N10	1.35	N16-N17	1.29		
	N10-H4	1.01	N17-N18	1.35		
	N10-C4	1.34	N18-H6	1.01		
	C2-N5	1.37	N18-C6	1.34		
	N5-H2	1.02				

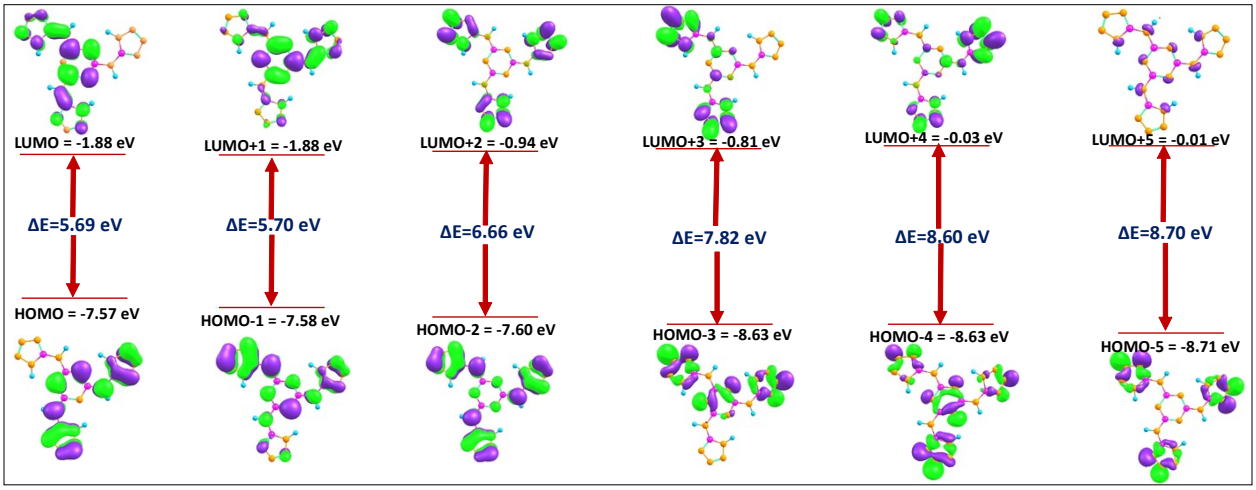

Fig. S23: HOMO-LUMO energy orbitals of gelator molecule **G8** studied by DFT analysis.

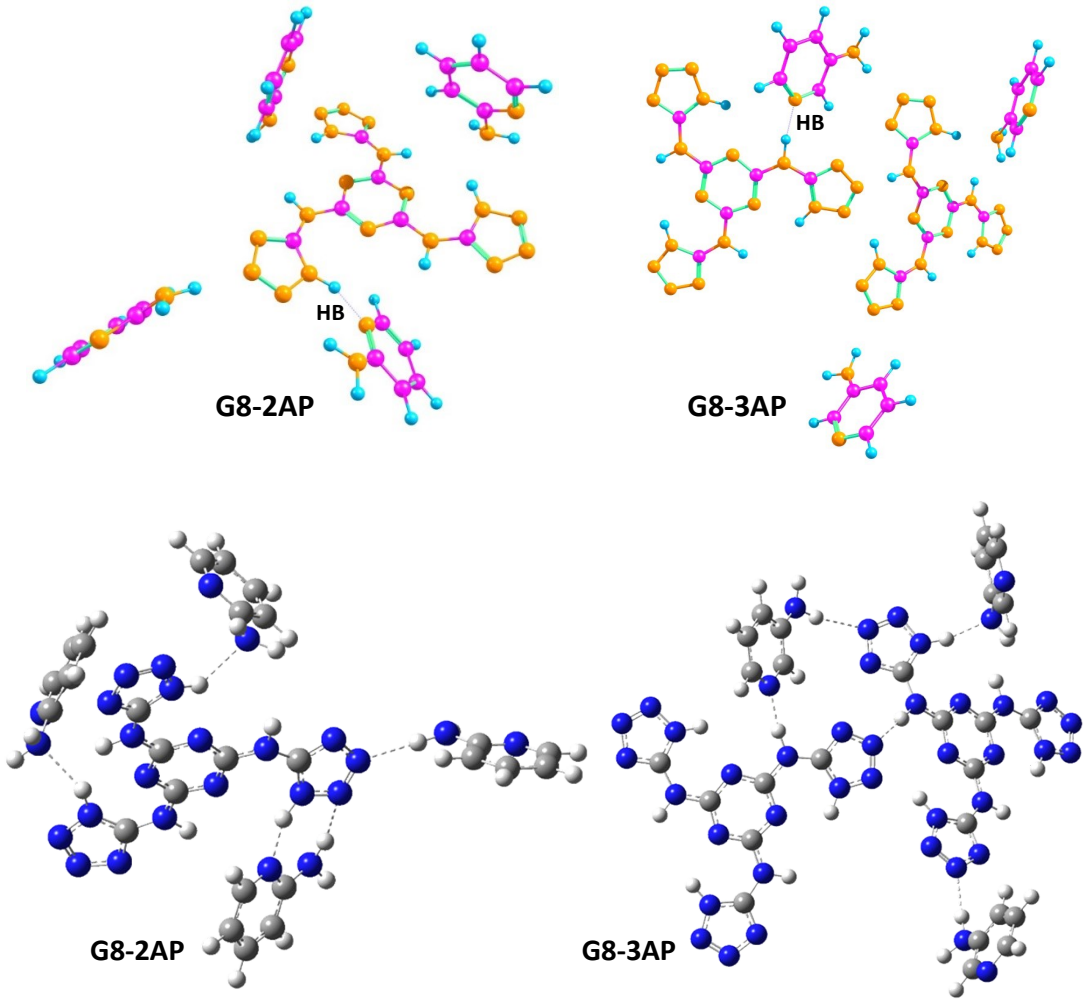

Fig. S24: Predicted structure demonstration of organogel **G8-2AP and G8-3AP** by DFT study.

Table S5: Comparative study of rheology of organogels **G8**, **G8-2AP**, **G8-3AP** and **G8-4AP**.

Gel	Value of storage modulus in Pa (in AS)	Value of storage modulus in Pa (in FS)	Value of storage modulus in Pa (in 3iTT)	Changes in storage modulus in Pa (From-to)
G8	2.16×10^2	2.36×10^2	3.96×10^2	3.96×10^2
G8-2AP	0.64×10^2	0.90×10^2	0.80×10^2	0.80×10^2
G8-3AP	5.02×10^3	5.14×10^3	4.46×10^3	4.46×10^3-7.74×10^2
G8-4AP	5.18×10^2	6.07×10^2	2.91×10^3	2.91×10^3 -1.91×10^3

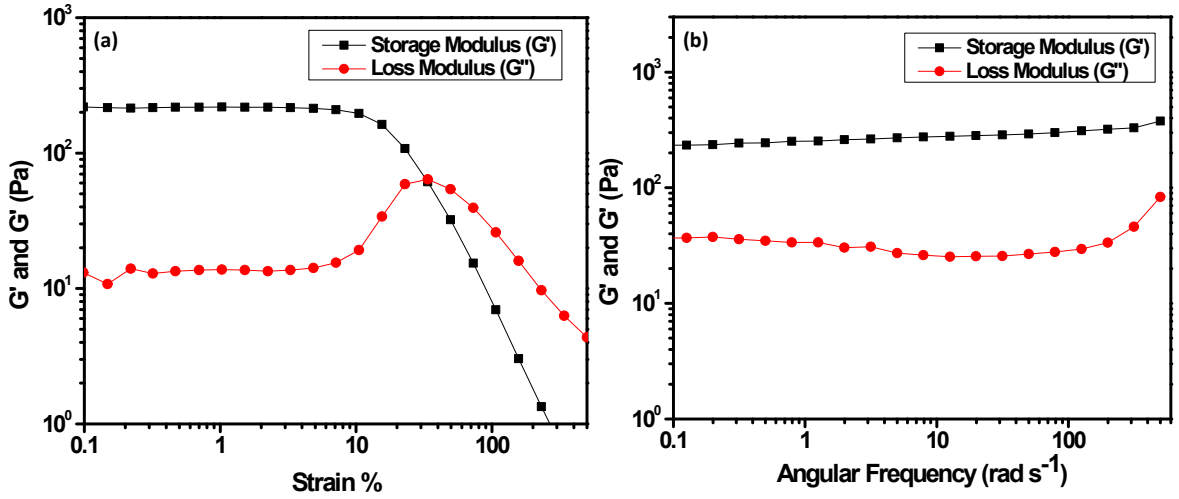

Fig. S25: (a) LVE Angular sweep (AS) and (b) Frequency sweep (FS) of organogel **G8**.

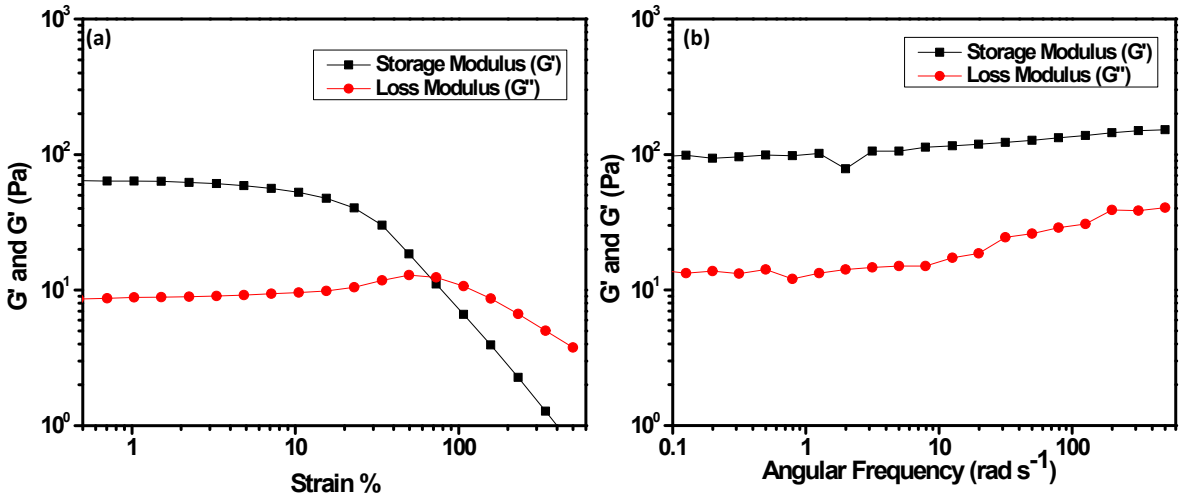

Fig. S26: (a) LVE Angular sweep (AS) and (b) Frequency sweep (FS) of organogel **G8-2AP**.

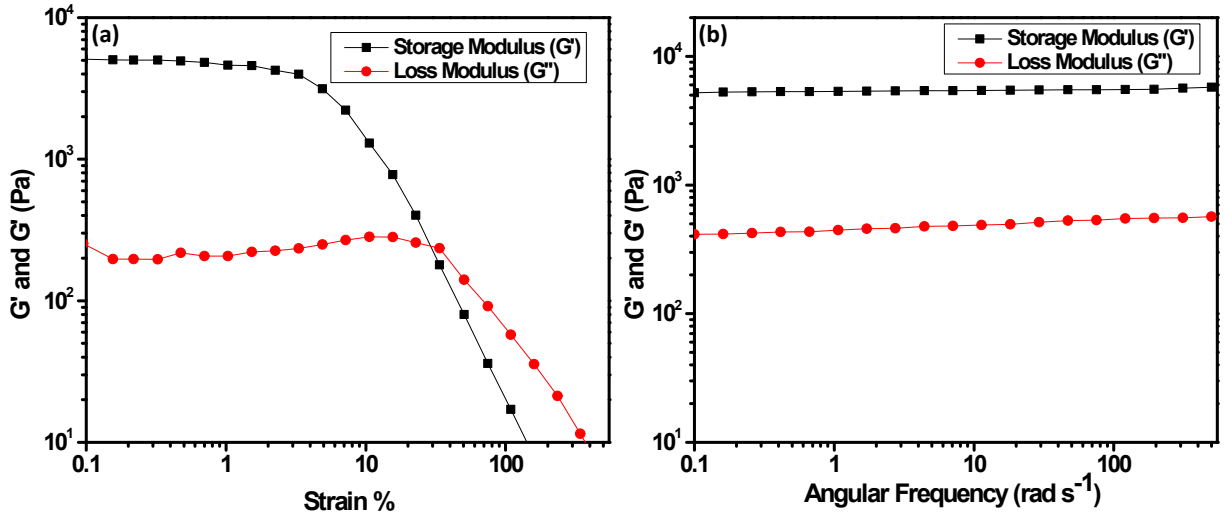

Fig. S27: (a) LVE Angular sweep (AS) and (b) Frequency sweep (FS) of organogel **G8-3AP**.

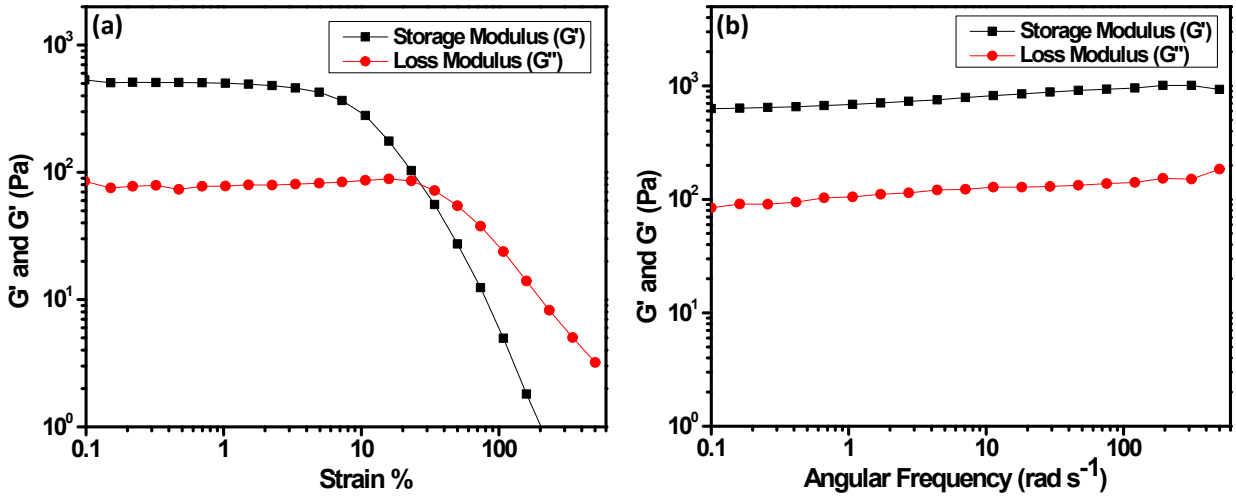

Fig. S28: (a) LVE Angular sweep (AS) and (b) Frequency sweep (FS) of organogel **G8-4AP**.

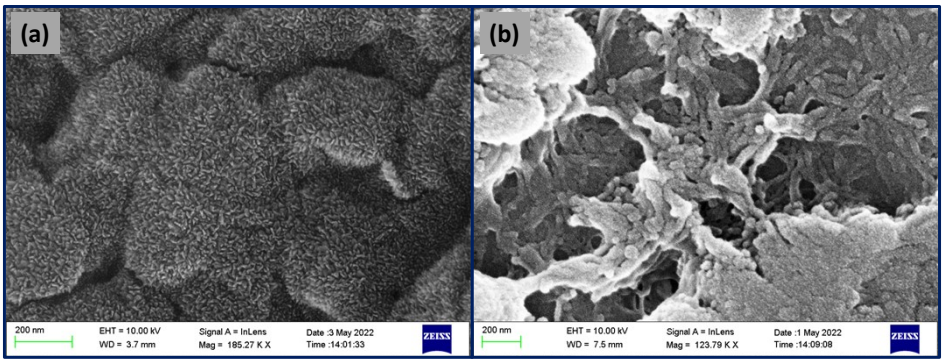

Fig. S29: FE-SEM images of (a) Organogel **G8** and (b) Xerogel of Organogel **G8** at 200 nm.

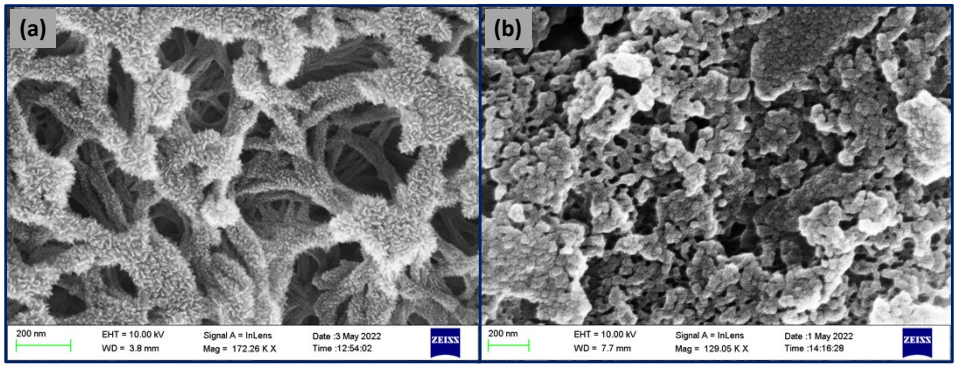

Fig. S30: FE-SEM images of (a) Organogel **G8-2AP** and (b) Xerogel of Organogel **G8-2AP** at 200 nm.

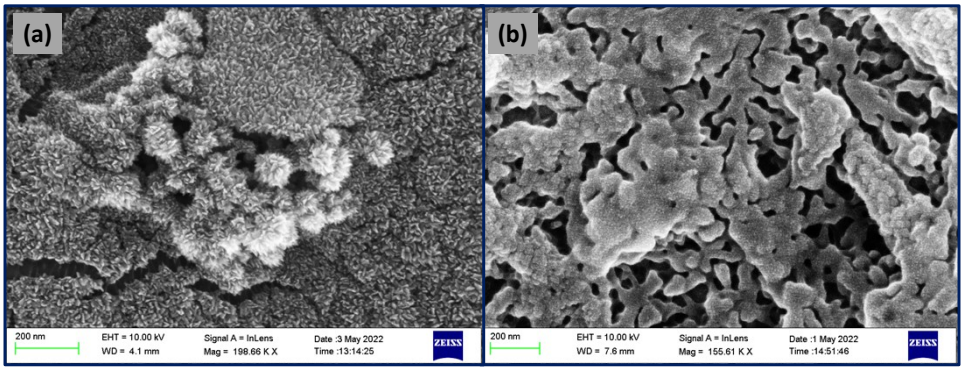

Fig. S31: FE-SEM images of (a) Organogel **G8-3AP** and (b) Xerogel of Organogel **G8-3AP** at 200 nm.

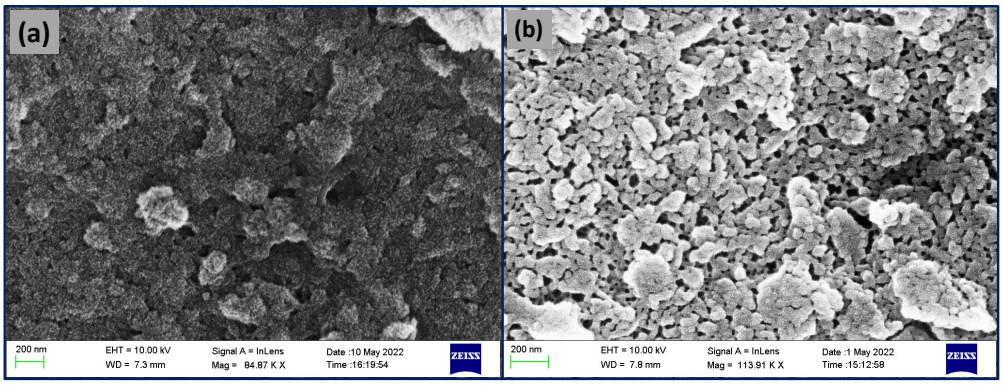

Fig. S32: FE-SEM images of (a) Organogel **G8-4AP** and (b) Xerogel of Organogel **G8-4AP** at 200 nm.

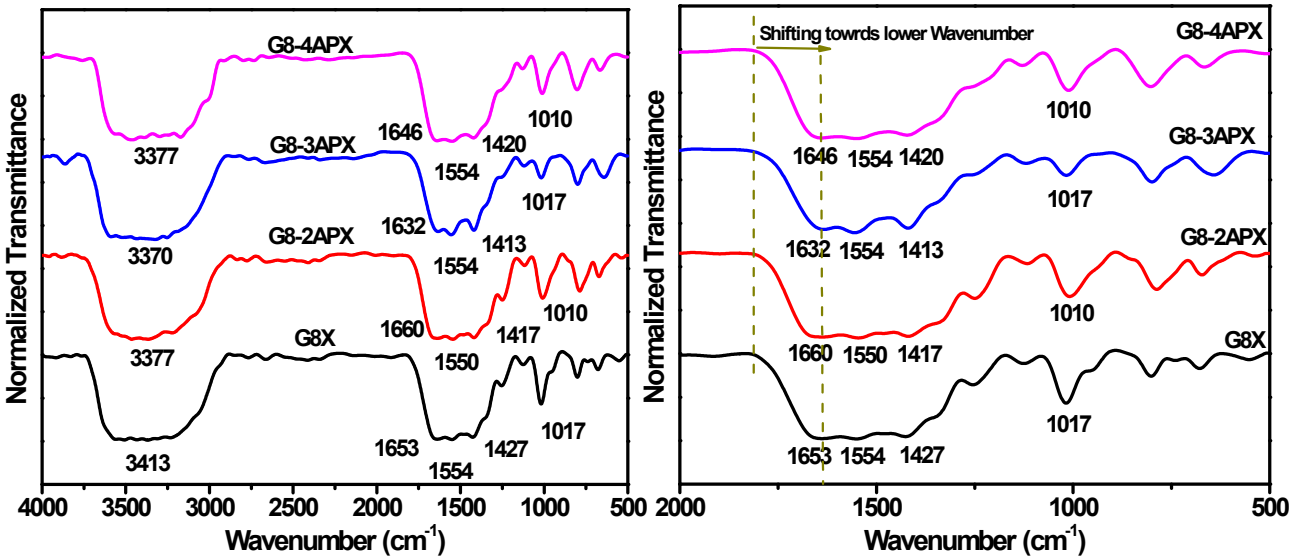

Fig. S33: FT-IR data of xerogel of **G8**, **G8-2APX**, **G8-3APX** and **G8-4APX**.

Table S6: Comparative wavenumber range to show the participation of amine and tetrazolic ring for gelation.

Gel	N-H Stretching (cm^{-1})	N-H Bending (cm^{-1})	C-N Stretching (aromatic amine) (cm^{-1})	C-N Stretching (amine) (cm^{-1})	C=N Stretching (imine) (cm^{-1})
G8-X	3413	1653	1427	1017	1554
G8-2AP	3377	1660	1427	1010	1550
G8-3AP	3370	1632	1413	1017	1554
G8-4AP	3377	1646	1420	1010	1554

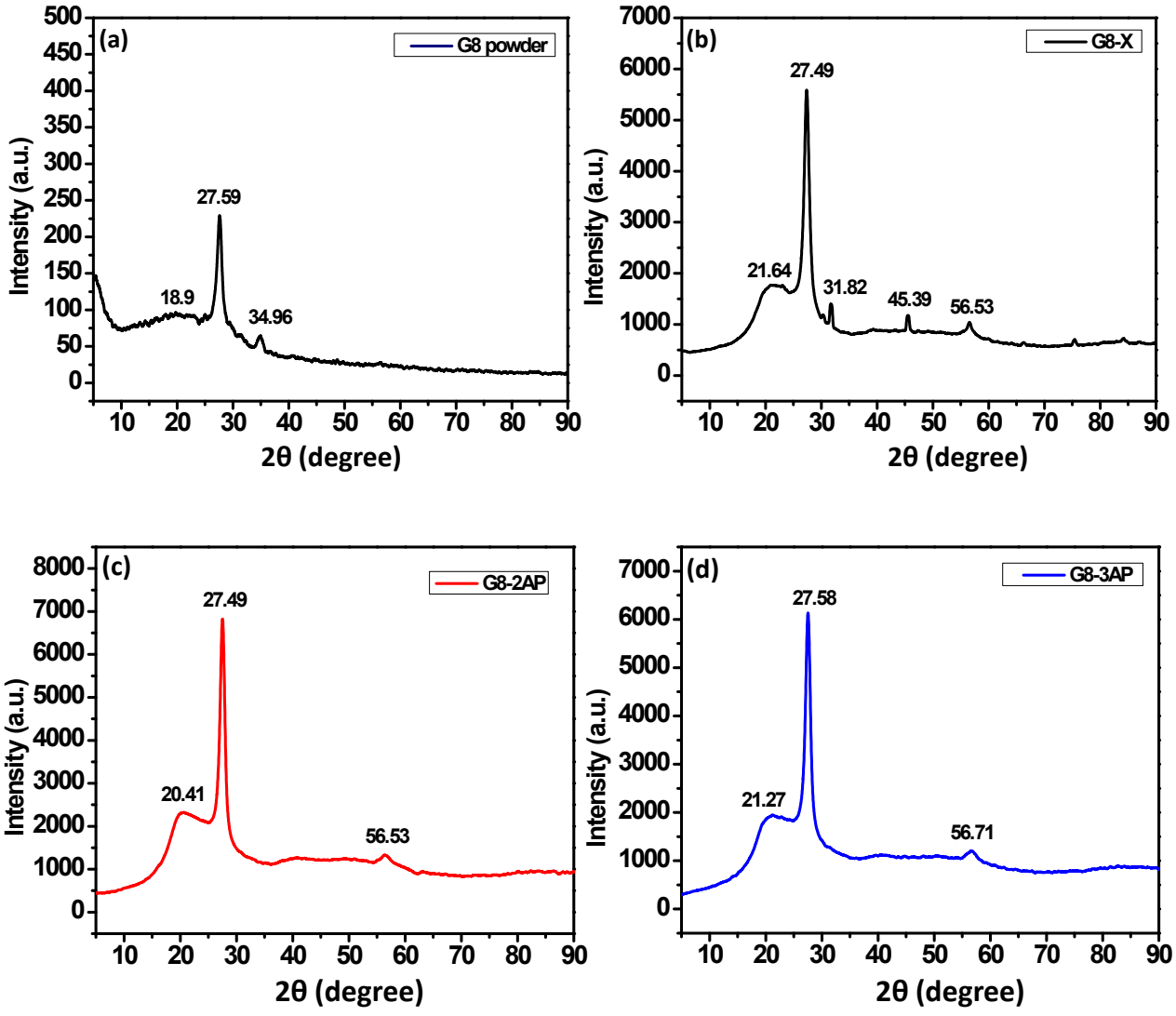

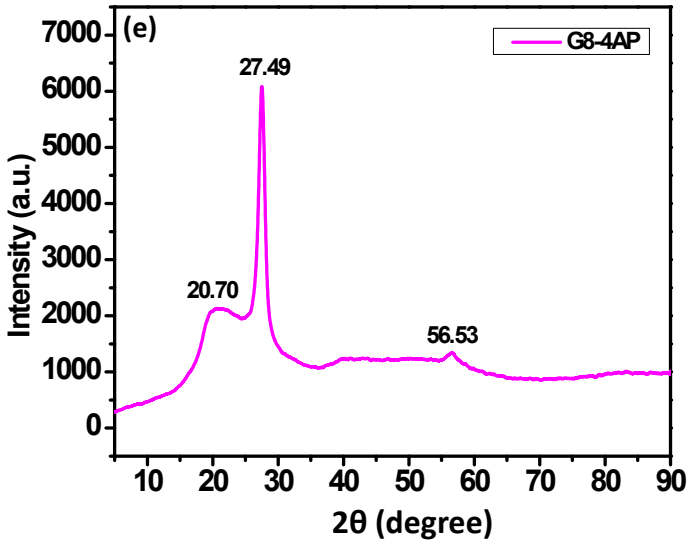

Fig. S34: PXRD data of (a) gelator powder **G8** and Xerogel of (b) **G8**, (c) **G8-2AP**, (d) **G8-3AP**, (e) **G8-4AP**.

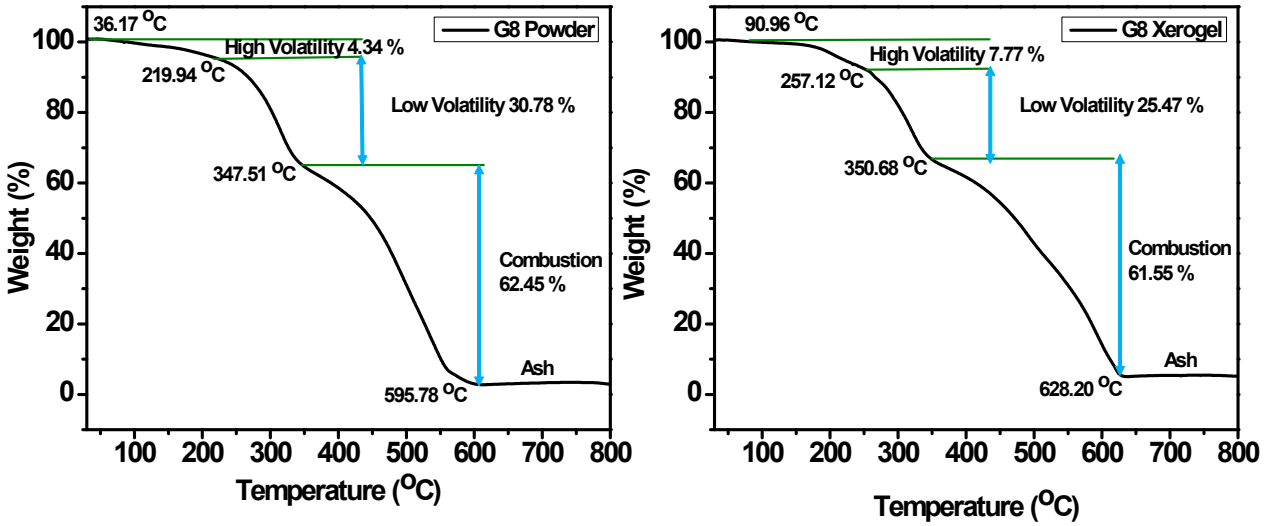

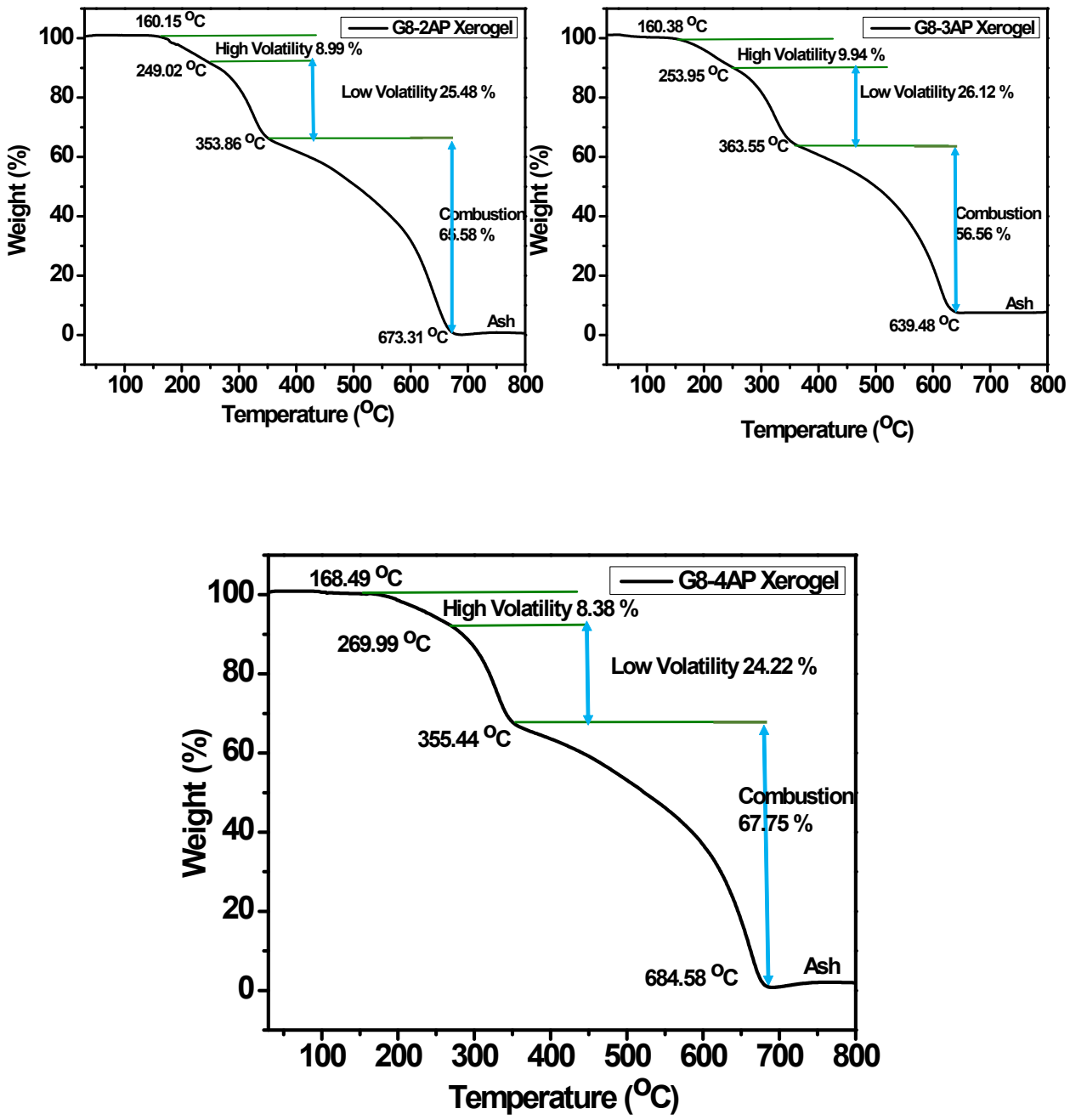

Fig. S35: TGA data of gelator molecule G8 and xerogels of organogels of **G8**, **G8-2AP**, **G8-3AP** and **G8-4AP**.